Applied Geochemistry 90 (2018) 75–86

Contents lists available at ScienceDirect

Applied Geochemistry

journal homepage: www.elsevier.com/locate/apgeochem

Mapping of bioavailable strontium isotope ratios in France for archaeological provenance studies

Malte Willmes[a,b,*], Clement P. Bataille[c], Hannah F. James[a], Ian Moffat[a,d], Linda McMorrow[a], Leslie Kinsley[a], Richard A. Armstrong[a], Stephen Eggins[a], Rainer Grün[a,e]

[a] Research School of Earth Sciences, The Australian National University, Bldg. 142 Mills Rd, Canberra 2602, ACT, Australia
[b] Department of Wildlife, Fish, and Conservation Biology, 1088 Academic Surge, One Shields Avenue, University of California Davis, 95616 Davis, CA, USA
[c] Department of Earth and Environmental Sciences, University of Ottawa, Ottawa K1N 6N5 Canada
[d] Department of Archaeology, Flinders University, Bedford Park, 5042 Adelaide, SA, Australia
[e] Australian Research Centre for Human Evolution, Environmental Futures Research Institute, Griffith University, 170 Kessels Road, Nathan, Queensland 4111, Australia

ARTICLE INFO

Editorial handling by Philippe Negrel.

Keywords:
Strontium isotopes
Tracing
Provenance
Plants
Soil leachates
Migration
Mobility

ABSTRACT

Strontium isotope ratios ($^{87}Sr/^{86}Sr$) of archaeological samples (teeth and bones) can be used to track mobility and migration across geologically distinct landscapes. However, traditional interpolation algorithms and classification approaches used to generate Sr isoscapes are often limited in predicting multiscale $^{87}Sr/^{86}Sr$ patterning. Here we investigate the suitability of plant samples and soil leachates from the IRHUM database (www.irhumdatabase.com) to create a bioavailable $^{87}Sr/^{86}Sr$ map using a novel geostatistical framework. First, we generated an $^{87}Sr/^{86}Sr$ map by classifying $^{87}Sr/^{86}Sr$ values into five geologically-representative isotope groups using cluster analysis. The isotope groups were then used as a covariate in kriging to integrate prior geological knowledge of Sr cycling with the information contained in the bioavailable dataset and enhance $^{87}Sr/^{86}Sr$ predictions. Our approach couples the strengths of classification and geostatistical methods to generate more accurate $^{87}Sr/^{86}Sr$ predictions (Root Mean Squared Error = 0.0029) with an estimate of spatial uncertainty based on lithology and sample density. This bioavailable Sr isoscape is applicable for provenance studies in France, and the method is transferable to other areas with high sampling density. While our method is a step forward in generating accurate $^{87}Sr/^{86}Sr$ isoscapes, the remaining uncertainty also demonstrates that fine-modelling of $^{87}Sr/^{86}Sr$ variability is challenging and requires more than geological maps for accurately predicting $^{87}Sr/^{86}Sr$ variations across the landscape. Future efforts should focus on increasing sampling density and developing predictive models to further quantify and predict the processes that lead to $^{87}Sr/^{86}Sr$ variability.

1. Introduction

Reconstructing past mobility patterns and land-use are crucial parts of understanding prehistoric societies, but it is complicated by the fact that the archaeological evidence becomes scarcer with time. The application of stable isotopes in archaeological research has revolutionised palaeomobility studies by providing independent data, which can be used to evaluate models of migration, trade, and cultural change. Strontium isotope ratios ($^{87}Sr/^{86}Sr$) have proven themselves to be a powerful tracer of provenance and mobility in a wide range of fields such as archaeology, ecology, food and forensic sciences (Beard and Johnson, 2000; Bentley, 2006; Hobbs et al., 2005; Kelly et al., 2005; Slovak and Paytan, 2012; Voerkelius et al., 2010; West et al., 2010).

The underlying principle is that $^{87}Sr/^{86}Sr$ ratios vary between different geologic regions as a function of bedrock age and composition (Faure and Mensing, 2005). Strontium is released by weathering of bedrock into the soils, ground and surface waters, from which it becomes available for uptake by plants and enters the food cycle (Bentley, 2006; Capo et al., 1998). Through their diet strontium is taken up by animals and humans and substitutes for calcium in biological apatite (bones, teeth), where it serves no metabolic function. Consequently, the $^{87}Sr/^{86}Sr$ ratio measured in a bone or tooth, will reflect the average of dietary Sr, that was consumed while the skeletal tissue was forming (Beard and Johnson, 2000; Bentley, 2006). Thus, $^{87}Sr/^{86}Sr$ ratios can be used to reconstruct changes in food sources and by extension residence area by comparing the values obtained from skeletal tissue with a baseline map of strontium isotopic variation across a region (e.g., Bentley, 2006; Slovak and Paytan, 2012.

A complicating factor is that the $^{87}Sr/^{86}Sr$ ratio of Sr available to

* Corresponding author. Department of Wildlife, Fish, and Conservation Biology, 1088 Academic Surge, One Shields Avenue, University of California Davis, 95616 Davis, CA, USA.
E-mail address: mwillmes@ucdavis.edu (M. Willmes).

https://doi.org/10.1016/j.apgeochem.2017.12.025
Received 13 September 2017; Received in revised form 22 December 2017; Accepted 27 December 2017
Available online 30 December 2017
0883-2927/

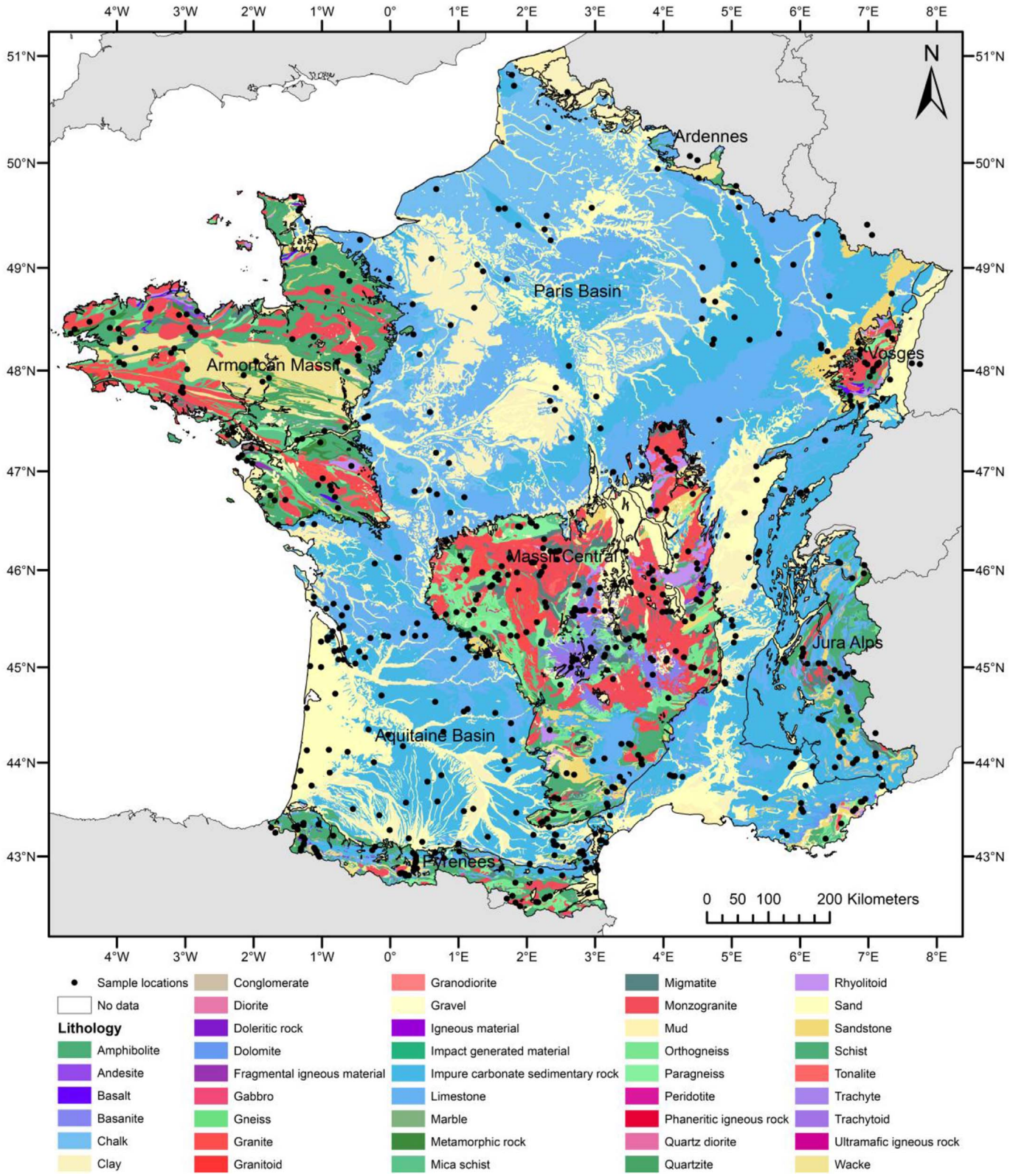

Fig. 1. Surface geologic map of France (BRGM) with sample sites from the IRHUM dataset marked as black dots.

biological organisms (termed bioavailable strontium) can differ from the bulk $^{87}Sr/^{86}Sr$ isotopic composition of the bedrock, due to the preferential weathering of certain minerals with different $^{87}Sr/^{86}Sr$ ratios (Sillen et al., 1998). In addition, the isotopic composition of the bioavailable strontium can be influenced by atmospheric deposition (precipitation, sea spray, dust), the presence of exogenous surface deposits (loess, glacial till, cover sands, peat), mixing processes between different strontium reservoirs, and anthropogenic influences such as fertilizer application and air pollution (Bentley, 2006; Evans et al., 2010; Frei and Frei, 2013; Maurer et al., 2012; Price et al., 2002; Slovak and Paytan, 2012; Widga et al., 2017). These processes vary between different areas and may introduce significant shifts in the bioavailable

$^{87}Sr/^{86}Sr$ ratio compared to the expected values based on bedrock geology.

Consequently, a variety of samples types have been used to create baseline bioavailable $^{87}Sr/^{86}Sr$ maps including rock leachates, soil leachates, plant samples, surface and ground water samples, archaeological and modern fauna or human remains (Bentley, 2006; Evans et al., 2009; Evans and Tatham, 2004; Maurer et al., 2012; Price et al., 2002; Slovak and Paytan, 2012). The best suited sample material for archaeological provenance studies are samples with the same food source range as the samples in question, such as well-preserved teeth with a known local origin (e.g. rodents). However, these are not available for large-scale (e.g. country wide) studies and thus substitute sample materials are needed. Despite this, no consensus currently exists in the literature as to what type of sample material is best suited to determine the overall spatial variability of bioavailable $^{87}Sr/^{86}Sr$ isotope ratios for a country wide study.

Terrestrial baseline $^{87}Sr/^{86}Sr$ ratio maps using different sample types and modelling methods have been produced for a number of regions at varying scales and spatial resolutions, for example for Europe (Voerkelius et al., 2010), Britain (Evans et al., 2010, 2009), Denmark (Frei and Frei, 2011, 2013), Netherlands (Kootker et al., 2016), Israel (Hartman and Richards, 2014), the contiguous USA (Bataille and Bowen, 2012; Beard and Johnson, 2000), Alaska (Bataille et al., 2014; Brennan et al., 2014), the Caribbean region (Bataille et al., 2012; Laffoon et al., 2012), Mesoamerica (Hodell et al., 2004), Puerto Rico (Pestle et al., 2013), South Africa (Copeland et al., 2016; Sillen et al., 1998), and South Korea (Song et al., 2014). In addition, archaeological provenance studies on smaller spatial scales have been carried out in many areas around archaeological sites producing local baseline maps (Bentley, 2006; Price et al., 2004, 2002; Slovak and Paytan, 2012).

Currently, only limited baseline $^{87}Sr/^{86}Sr$ data exists for France, hindering the use of $^{87}Sr/^{86}Sr$ ratios for investigating the provenance of samples from the vast archaeological record in France. The aim of this study is to build on the previously published dataset of $^{87}Sr/^{86}Sr$ ratios of plants and soil leachates (Willmes et al., 2014) to produce a bioavailable $^{87}Sr/^{86}Sr$ baseline map for archaeological provenance studies for continental France.

2. Data and methods

2.1. Sample selection

The IRHUM (Isotopic Reconstruction of Human Migration) database is a web platform for sharing and mapping $^{87}Sr/^{86}Sr$ ratios from environmental samples (Willmes et al., 2014). For continental France, it presently contains 843 sample locations from which plant samples and top soil leachates have been analysed for $^{87}Sr/^{86}Sr$ ratios (Pangaea data repository http://dx.doi.org/10.1594/PANGAEA.819142, www.irhumdatabase.com). The analytical methods are described in detail in Willmes et al. (2014). In brief, plant samples are considered to represent a direct measure of bioavailable Sr and were ashed and completely dissolved. Soil samples were subjected to a ammonium nitrate (NH_4NO_3) leaching process to extract the bioavailable part of the bulk strontium (Capo et al., 1998; Gryschko et al., 2005; Hall et al., 1998; Meers et al., 2007; Prohaska et al., 2005; Rao et al., 2008; Sillen et al., 1998). Sr concentrations and $^{87}Sr/^{86}Sr$ ratios were measured at the Research School of Earth Sciences (RSES). We selected 610 sample locations from the dataset, which cover all major geologic units and lithologies of France (Fig. 1). This subset of the IRHUM dataset excludes sample locations that are situated on geologic units that are not characteristic for their geographic area, such as minor geologic outcrops ($< 10\,km^2$), river terraces, as well as sample sites that are likely to represent modern anthropogenic activity, such as agricultural fields and managed forest areas.

2.2. Spatial and statistical methods

The strontium isotope data from the IRHUM database were spatially joined with the geologic map of France (Chantraine et al., 2005) and the surface geologic map of France (BRGM) using ESRI ArcGIS™. The definitions of the lithological units are taken from the OneGeology-Europe project (http://www.onegeology-europe.org). The data were then screened to check that the described lithology from the IRHUM dataset matches the lithology from the geologic maps. In case of discrepancies the lithology was matched to the closest corresponding geological unit. Finally, we removed minor lithological units from the data (e.g. impact generated rocks, mud, amphibols, quartzites) and simplified and merged the lithological information to achieve uniform descriptions of units across France. For non-parametric statistical analysis Microsoft Excel and R (R Core Team, 2017) were used. For the box and whisker plot the top and bottom of the box are defined as the third and first quartiles. The interquartile range (IQR) is calculated by subtracting the first quartile from the third. The second quartile, which is the median, is shown as a black line. The whiskers are defined as Q1-1.5*IQR for the lower whisker and Q3 + 1.5*IQR for the upper whisker. Cluster analysis was conducted using R with the cluster (Maechler et al., 2015), fpc (Hennig, 2015), and clValid (Brock et al., 2008) packages.

2.3. Kriging methods

Kriging is a geostatistical interpolation method, which depends on statistical models of spatial autocorrelation (Goovaerts, 1998; Krige, 1951; Saby et al., 2006). Briefly, the trends in spatial autocorrelation between pairs of points from a given dataset are modelled by fitting a curve or “variogram model”. This variogram model is then used as a basis to interpolate the target variable away from the points. Several versions of kriging have been developed but in this study, we focus on ordinary kriging and kriging with external drift. Ordinary kriging is the most commonly used, it predicts a value at any given location by using the local mean and a variogram model of the spatial autocorrelation. Kriging with external drift is similar but instead of using the local mean, it estimates a trend based on an auxiliary predictor, and solves simultaneously for second order effects. In this study, we use the map of isotope groups derived from the cluster analysis as the primary auxiliary variable in the kriging with external drift approach. All kriging was carried out separately for soil and plant samples using the geostatistical toolbox in ArcGIS (ESRI). Both soil and plant data are evaluated separately and in addition a combined soil and plant layer is generated by averaging the two original geostatistical layers (predictions and estimated errors) using the raster toolbox in ArcGIS (ESRI).

3. Results and discussion

3.1. Comparison of strontium isotope ratios in plant and soil samples

In theory, both soil leachates, which represent the bioavailable Sr of the soil, and plant samples, which are a direct measure of the bioavailable Sr, should result in similar $^{87}Sr/^{86}Sr$ ratios at a given sample location (Blum et al., 2000; Hodell et al., 2004). 499 sample locations in this study contain data for both plant samples and soil leachates and thus can be used to investigate potential differences between these sample types. We define the difference between plant samples and soil leachates as $\Delta_{PS} = (^{87}Sr/^{86}Sr_{plant} - {}^{87}Sr/^{86}Sr_{soil\ leachate})$. Overall, we find a strong positive correlation between the plant and soil $^{87}Sr/^{86}Sr$ ratios ($R = 0.94$). The average Δ_{PS} value, calculated from absolute values, is 0.0008 ± 0.0012 (σ, $n = 499$), median is 0.0002. However, some sample sites show a significantly higher offset between plant and soil samples. The largest Δ_{PS} is -0.0085, which encompasses a large part of the entire $^{87}Sr/^{86}Sr$ ratio variation of France at a single sample location. Sites with large Δ_{PS} values show that soil and plant samples collected in very close spatial context can still represent vastly different strontium

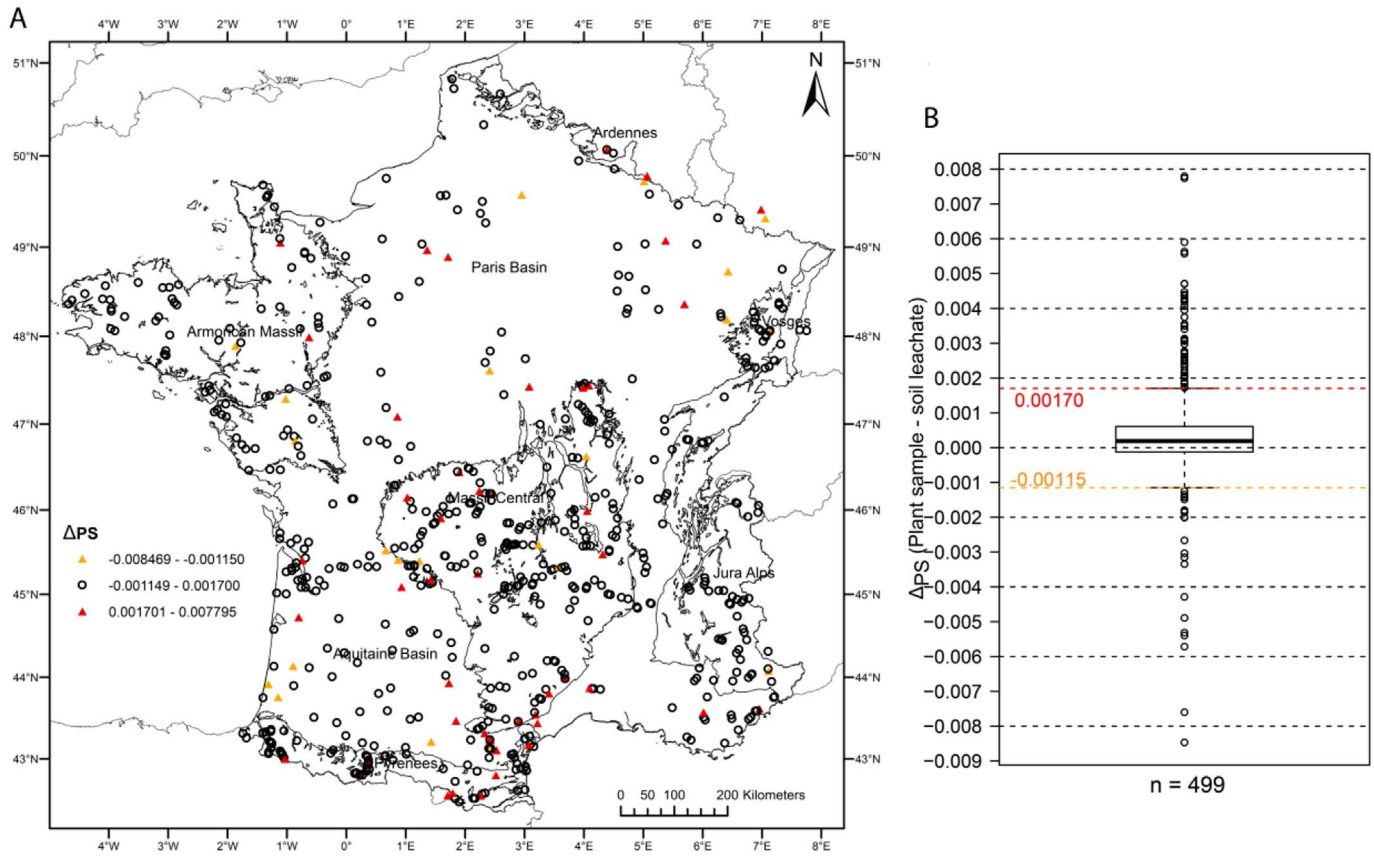

Fig. 2. A: Geographic distribution of Δ_{PS} values in France and B: Boxplot of the Δ_{PS} values. Outliers are defined by the whiskers, as any value higher than 0.00170 and lower than −0.00115.

isotope reservoirs (Fig. 2). This has been observed in previous studies (Blum et al., 2000; Evans et al., 2010; Evans and Tatham, 2004; Hodell et al., 2004; Maurer et al., 2012), and can result from a multitude of different processes.

The primary driver for $^{87}Sr/^{86}Sr$ isotopic variation across a landscape is the underlying geology and thus differences in Δ_{PS} may also be related to difference between lithologies. Soils and plants in geologically complex areas may form on geochemically highly mixed substrates, caused by the weathering of different rock types and different minerals within the same rock (e.g., Sillen et al., 1998). Thus, lithological complex units (e.g., gravels, granites, orthogneisses) are expected to show higher average Δ_{PS} values than geochemical homogenous lithological units (e.g., limestones). For example, we find high Δ_{PS} values for gravel units that could reflect their heterogeneous composition consisting of rock fragments with potentially vastly different $^{87}Sr/^{86}Sr$ ratios placed next to each other. However, in contrast to this hypothesis, the average Δ_{PS} values of limestones and granites are similar (Table 1). The majority of soils are not only the product of *in situ*

Table 1
Summary statistics of the Δ_{PS} values for the different lithological units. Δ_{PS} values are calculated as absolute values, ignoring the direction of the offset between the sample types.

Δ_{PS} (plant sample-soil leachate)						Outlier		
Lithologies	Min	Max	Average	Sample pairs [n]	1σ	Sample pairs [n]	%	Outlier removed average Δ_{PS}
Volcanics (Basanites, Tephrites, Pyroclastica, Trachytes)	0.00001	0.00065	0.00022	22	0.00017	0	0	0.00022
Chalk	0.00006	0.00563	0.00147	6	0.00213	2	33	0.00034
Dolomite	0.00013	0.00047	0.00028	4	0.00014	0	0	0.00028
Limestone	0.00001	0.00557	0.00066	67	0.00107	6	9	0.00036
Impure carbonate sedimentary rock	0.00001	0.00471	0.00079	95	0.00094	14	15	0.00047
Clay	0.00002	0.00760	0.00096	26	0.00160	5	19	0.00036
Sand	0.00000	0.00774	0.00082	52	0.00132	8	15	0.00041
Gravel	0.00023	0.00531	0.00207	5	0.00217	2	40	0.00023
Conglomerate	0.00006	0.00572	0.00128	15	0.00176	4	27	0.00036
Sandstone	0.00007	0.00429	0.00094	20	0.00111	4	20	0.00047
Wacke	0.00010	0.00066	0.00031	3	0.00031	0	0	0.00031
Granite	0.00001	0.00847	0.00067	64	0.00119	4	6	0.00043
Paragneiss	0.00001	0.00145	0.00048	15	0.00037	0	0	0.00048
Orthogneiss	0.00001	0.00437	0.00096	19	0.00100	3	16	0.00073
Migmatite	0.00005	0.00590	0.00091	15	0.00150	2	13	0.00041
Schist	0.00002	0.00780	0.00113	55	0.00155	12	22	0.00045
Mica schist	0.00006	0.00090	0.00038	5	0.00039	0	0	0.00038
Rhyolitoid	0.00015	0.00375	0.00130	11	0.00133	3	27	0.00055
All lithologies	0.00000	0.00847	0.00082	499	0.00123	70	14	0.00043

weathering but a composite of different processes and different strontium sources. Overall, we find high average Δ_{PS} values both in heterogeneous as well as in homogenous geologic substrates, indicating that the underlying geology is not the only driver for the observed difference between soil and plant samples.

Differences in $^{87}Sr/^{86}Sr$ values between top soil and plant samples are influenced by a plant's root depth, which may allow the sampling of soil horizons with differing $^{87}Sr/^{86}Sr$ values and the plant's susceptibility to atmospheric deposition of strontium (Drouet et al., 2007; Maurer et al., 2012; Poszwa et al., 2004, 2002). In this study, we concentrated on top soil samples and shallow rooted plants (grasses, shrubs). We dissolved the entire plant rather than specific tissues to mitigate this potential source of variability. Grasses should more closely reflect the $^{87}Sr/^{86}Sr$ ratio of the topsoil than other plant species with deeper roots. However, we observe high Δ_{PS} values for all plant sample types including grass samples (Fig. 3). There is no significant difference in average Δ_{PS} values for grass samples (mean = 0.00082, median = 0.00041, n = 380) compared to tree roots (mean = 0.00086, median = 0.00042, n = 35) and other plant sample types (mean = 0.00083, median = 0.00038, n = 84). The exception being moss samples that show higher average Δ_{PS} values (mean = 0.00107, median = 0.0046, n = 35). Finally, both soil and plant samples have a similar variance of 0.00002, indicating that the variability did not decrease as strontium was moved from the soil into the plant.

External input of strontium, such as precipitation, sea spray, and dust, can potentially create difference between sample materials. As a first order observation, we find no direct spatial correlation between the occurrence of Δ_{PS} values and precipitation and land use. However, these processes could not be investigated in detail because we are lacking the data to constrain the $^{87}Sr/^{86}Sr$ ratios of these sources.

Finally, on the scale of France, it is likely that at any given sample location a combination of the discussed processes is at work. Identification of the driver of Δ_{PS} values is confounded by the complex interplay between weathering of lithology, soil genesis, plant processes, and external strontium inputs that vary both in absolute strontium concentrations as well as isotope ratios, spatially and with time. Based solely on the strontium isotope ratios it is not possible to untangle these processes and quantification of external strontium inputs was beyond the scope of this work. We intend to revisit a range of sites to conduct detailed sampling to investigate the differences between plant samples and soil leachates. Concerning the aim of this study, which is to create a robust baseline map, we incorporated the observed local variability but excluded outlier sites that are not representative of their lithological unit and geographic area. This approach does not favour a specific sample material, taking into account that there are likely multiple processes at work that create the variations in $^{87}Sr/^{86}Sr$ ratios observed at specific sites. We classify outlier Δ_{PS} values based on the boxplot (Fig. 2) as any value above Q3 + 1.5 × IQR or below Q1–1.5 × IQR (+0.00170 and −0.00115, respectively). In total, 70 sample locations (~14%) have Δ_{PS} values outside of this range (Table 1). Removing these sample locations results in a dataset with an average Δ_{PS} value of 0.0004 ± 0.0004 (1σ, n = 429) and improves the correlation between

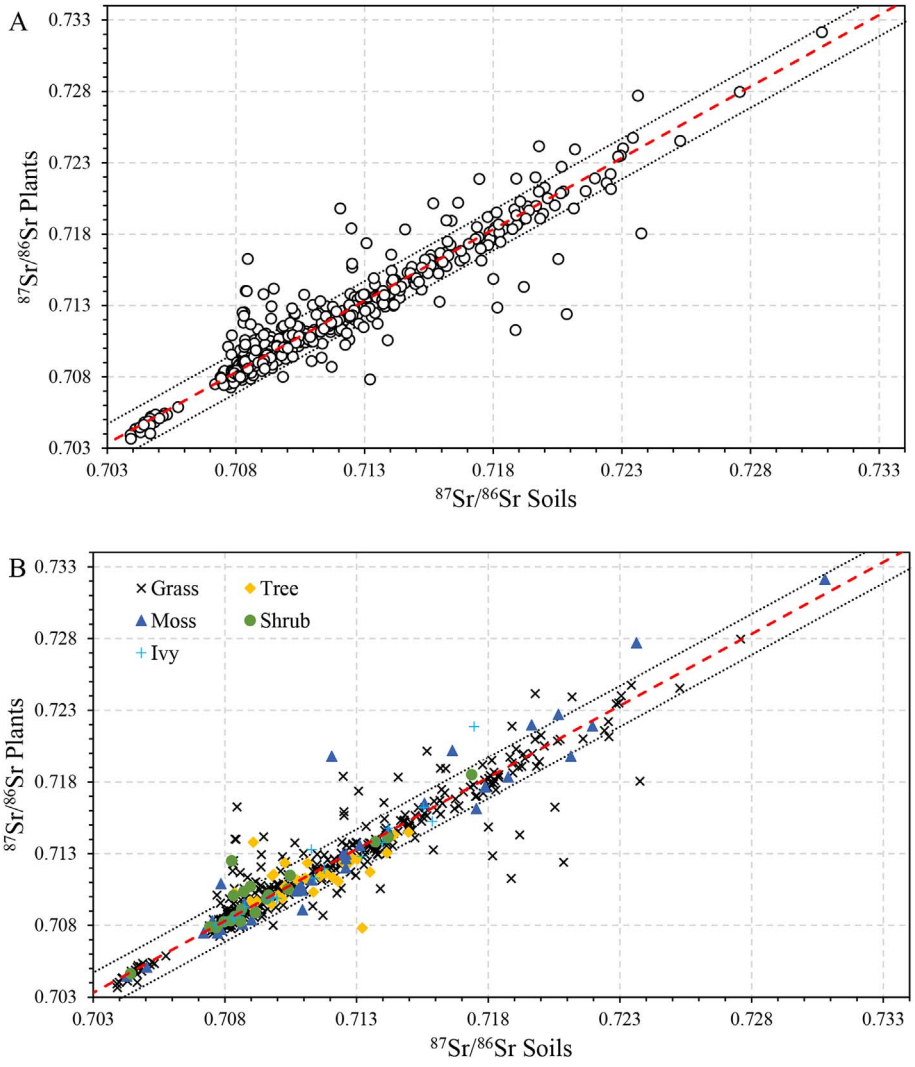

Fig. 3. $^{87}Sr/^{86}Sr$ ratios of plants plotted against soil leachate values from the same site. A: Plot including all sample pairs, a linear fit is shown in red. Grey lines are the top and bottom whisker from the boxplot of Δ_{PS} values (Fig. 2), and any data point outside of the grey lines is identified as an outlier. B, same data plotted as in A, classified based on plant type. (For interpretation of the references to colour in this figure legend, the reader is referred to the Web version of this article.)

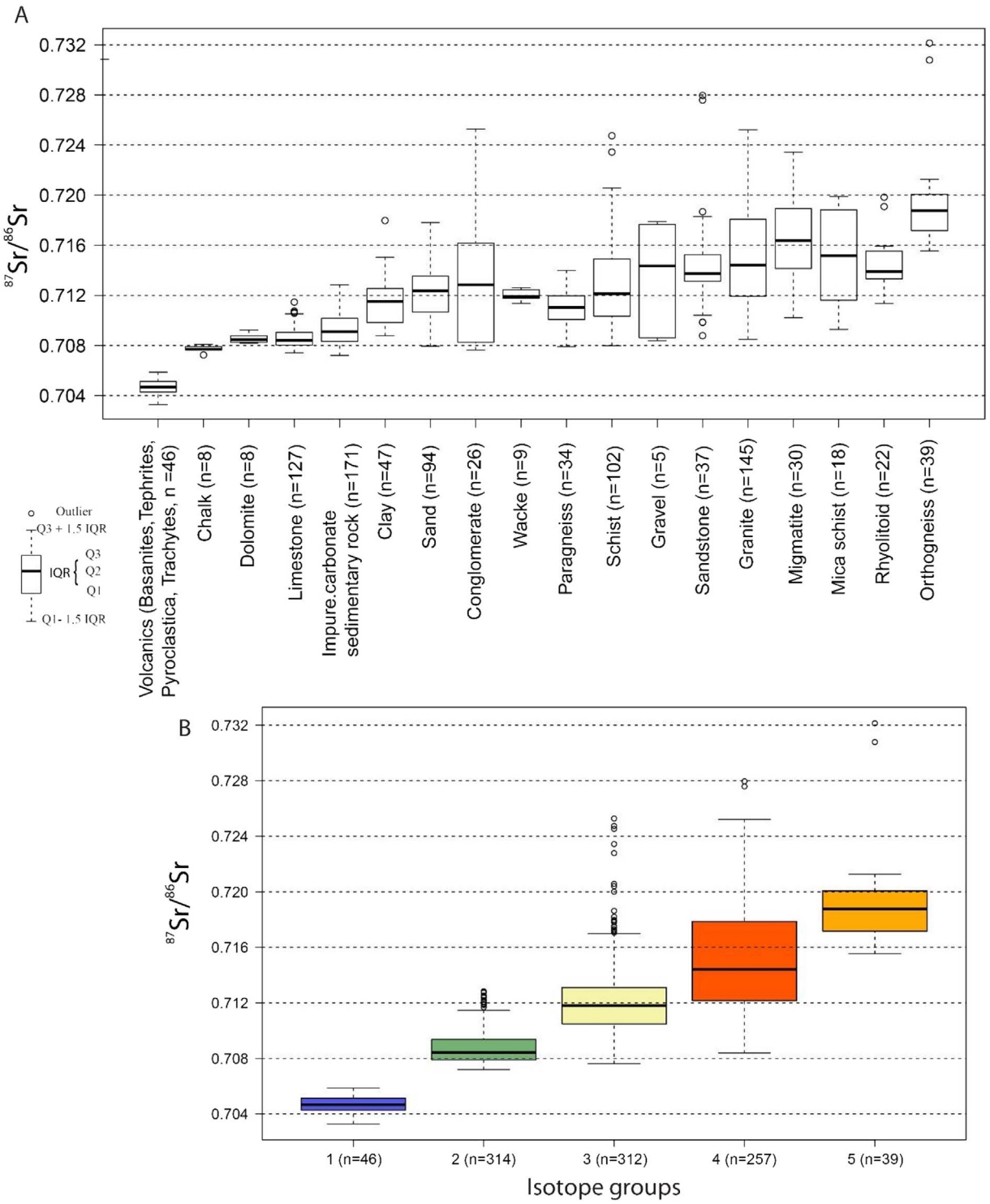

Fig. 4. Box and whisker plot of the bioavailable $^{87}Sr/^{86}Sr$ range, A for each lithology and B for the 5 isotope groups (n = number of samples). The isotope groups combine lithologies to minimize the internal variance and maximize the difference between groups.

plant and soil samples (R = 0.99). The risk in removing these sites is that it could potentially lead to an underestimation of the strontium isotopic variability for certain lithological units. We tested this by comparing the strontium isotope range for each lithological unit from the complete and the outlier removed dataset. No significant differences are observed, indicating that removing the outliers did not affect the overall strontium isotopic variability of the different lithological units. The exceptions are the gravel and chalk units, which show significantly narrower strontium isotope ranges after outlier removal. However, these lithologies are represented only by a small number of samples (gravel n = 5, chalk n = 8). The results for these two units should thus be treated with caution and specifically the gravel samples cannot be considered to represent the full strontium isotopic range of these units for France.

3.2. Strontium isotope groups

The dataset presented here consists of 540 sample locations, with a

Table 2
Summary statistics for the bioavailable $^{87}Sr/^{86}Sr$ range for each lithology and the isotope groups.

Lithologies	Isotope Group	Bioavailable $^{87}Sr/^{86}Sr$					n	Area [km^2]
		Q1-1.5*IQR	Q1	Q2	Q3	Q3 + 1.5*IQR		
Volcanics	1	0.70328	0.70428	0.70468	0.70514	0.70587	46	12693
Chalk	2	0.70764	0.70765	0.70770	0.70790	0.70808	8	100291
Dolomite	2	0.70818	0.70825	0.70846	0.70877	0.70923	8	5772
Limestone	2	0.70741	0.70802	0.70842	0.70904	0.71052	127	172254
Imp. carb. sedi. rock	2	0.70720	0.70832	0.70910	0.71017	0.71284	171	252846
Clay	3	0.70877	0.70983	0.71152	0.71253	0.71504	47	114622
Sand	3	0.70794	0.71067	0.71236	0.71354	0.71781	94	159230
Conglomerate	3	0.70763	0.70825	0.71284	0.71617	0.72528	26	2562
Wacke	3	0.71136	0.71177	0.71191	0.71244	0.71261	9	25385
Paragneiss	3	0.70790	0.71007	0.71104	0.71196	0.71399	34	20603
Schist	3	0.70799	0.71035	0.71214	0.71489	0.72057	102	75615
Gravel	4	0.70839	0.70862	0.71434	0.71766	0.71788	5	1800
Sandstone	4	0.71041	0.71312	0.71374	0.71525	0.71829	37	27438
Granite	4	0.70849	0.71193	0.71441	0.71808	0.72521	145	100313
Migmatite	4	0.71022	0.71414	0.71638	0.71893	0.72343	30	16332
Mica schist	4	0.70928	0.71161	0.71518	0.71883	0.71989	18	14434
Rhyolitoid	4	0.71135	0.71332	0.71390	0.71552	0.71593	22	9635
Orthogneiss	5	0.71555	0.71717	0.71876	0.72007	0.72126	39	18940
Isotope Group	1	0.70328	0.70428	0.70468	0.70514	0.70587	46	12693
	2	0.70720	0.70790	0.70842	0.70937	0.71147	314	531163
	3	0.70763	0.71048	0.71180	0.71311	0.71699	312	398017
	4	0.70839	0.71216	0.71441	0.71786	0.72521	257	169952
	5	0.71555	0.71717	0.71876	0.72007	0.72126	39	18940

total of 968 individual samples, after outlier removal. The bioavailable $^{87}Sr/^{86}Sr$ ratios for each lithological unit are shown in Fig. 4, Table 2, and significant overlap in $^{87}Sr/^{86}Sr$ ratios exists between different lithological units.

We performed cluster analysis to identify groups of lithological units with minimized internal variance and maximum difference between groups in $^{87}Sr/^{86}Sr$ ratios. Several different clustering techniques (hierarchal, k-means, pam) were tested and k-means clustering set to 5 clusters was found to produce the highest optimized values, as determined by cluster validation (optimal Silhouette and Dunn values). Bedrock age is often used as a classifier to group $^{87}Sr/^{86}Sr$ ratios as older and more rubidium rich rocks have higher $^{87}Sr/^{86}Sr$ ratios, but in this dataset lithology rather than age was found to be a better cluster variable. We grouped the lithological units and their strontium isotope ranges into 5 isotope groups. The contribution of each lithological unit to its isotope group was weighted by the relative area of that lithological unit.

We defined the following isotope groups:

- Isotope group 1 (0.7033–0.7059) includes the volcanic units (basanites, tephrites, trachytoids) predominantly found within the Massif Central.
- Isotope group 2 (0.7072–0.7115) is comprised of the carbonaceous sediments (chalk, dolomite, limestone, impure carbonate sedimentary rocks) and is the dominant lithology in the Aquitaine Basin, Paris Basin and Alpine Foreland.
- Isotope group 3 (0.7076–0.7170) comprises the clay, sand, conglomerate wacke, paragneiss, schist units. The clastic sediments are found within the basins along rivers intercutting the units of isotope group 2 as well as along the Atlantic coastline. Paragneiss and schist units are found in the mountainous regions with large outcrops in the Armorican Massif, Massif Central, and in the Pyrenees.
- Isotope group 4 (0.7084–0.7252) is composed of the gravel, sandstone, granite, migmatite, mica schist, and rhyolitoid units. These units are found dominantly in the mountainous regions of France.
- Isotope group 5 (0.7155–0.7213) includes the orthogneiss units found in the Massif Central and Pyrenees.

The isotope group map (Fig. 5) is a simplified representation of the bioavailable $^{87}Sr/^{86}Sr$ ranges of the lithological units and first strontium isotope baseline map for France. Since it is based on the surface geologic map it is accurate in displaying the sharp geologic boundaries and their corresponding changes in bioavailable $^{87}Sr/^{86}Sr$ ratios. Limitations of the map are that because lithology was used as classification it does not allow us to investigate isotopic variation within single lithological units. The large strontium isotope ranges and significant overlaps (Fig. 6) are a direct result of using the broad lithological units as classifiers for the isotope groups. For example, granites are represented as one unit, but different types of granites can have vastly different initial Rb concentrations and resulting $^{87}Sr/^{86}Sr$ ratios. A similar effect can be observed in the clastic sediments, which vary significantly in their $^{87}Sr/^{86}Sr$ ratios depending on their source region (e.g., between mountainous areas and the basins) but are here grouped together causing an increase in their internal variability. Consequently, the main limitation of this map is related to the high variability in $^{87}Sr/^{86}Sr$ ratios observed for many lithological units. This map can thus be used to identify broad geographic patterns of residence change, but may not resolve smaller scale mobility and land-use changes within similar $^{87}Sr/^{86}Sr$ isotopic regions. For example, isotope group 1 is constrained to a small area in the Massif Central and thus a sample with a corresponding isotope value could be placed into a tight geographic constrain, while samples with isotope values similar to isotope group 2 could correspond to many areas in the Paris and Aquitaine Basin. This reflects both the high variability found in isotope group 2 as well as the fact that distant geographic locations may exhibit closely similar $^{87}Sr/^{86}Sr$ ratios based on their similar underlying geology.

3.3. Kriging

Significant overlap in $^{87}Sr/^{86}Sr$ ratios exists between different lithological units, showing that the strontium isotope ratios form a continuum rather than specific readily distinguishable groups. To take this into account and to incorporate the variability in strontium isotope ratios within the larger geological units (used previously as classifiers) we performed kriging to interpolate the $^{87}Sr/^{86}Sr$ ratios between sample locations (Table 3). Kriging generates a smooth continuous surface and allows us to investigate more subtle changes in $^{87}Sr/^{86}Sr$ ratios within geologic units. We compared ordinary kriging and kriging

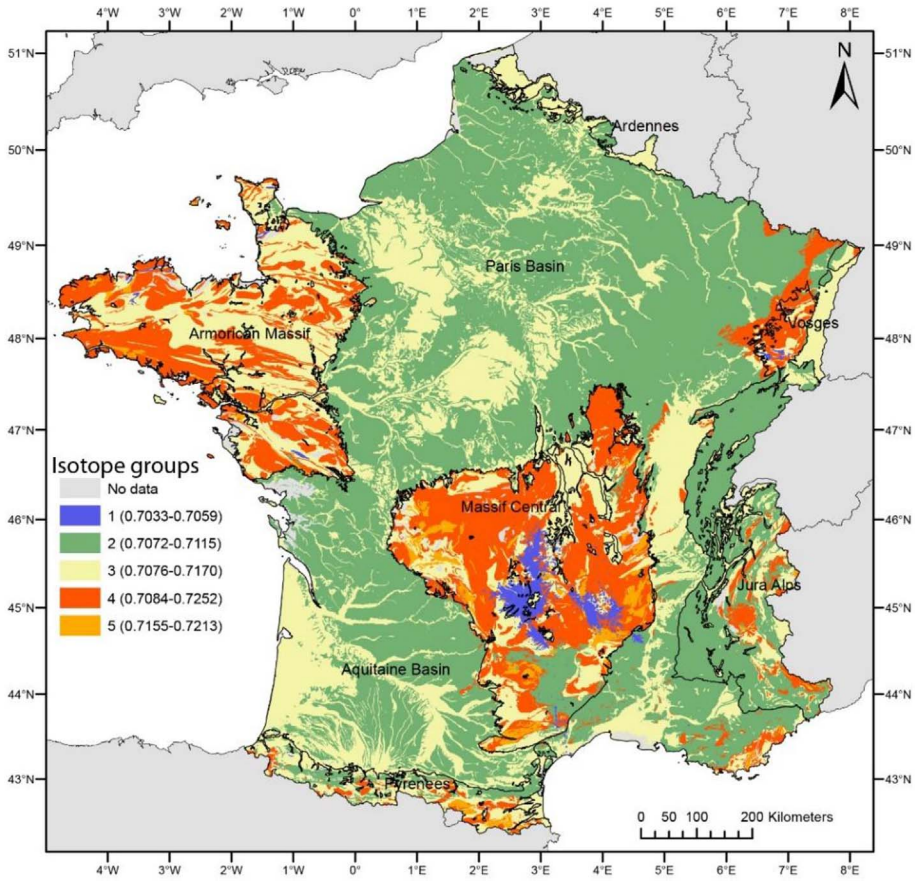

Fig. 5. Map of the surface geologic lithologies of France, coloured by their classification into the 5 isotope groups.

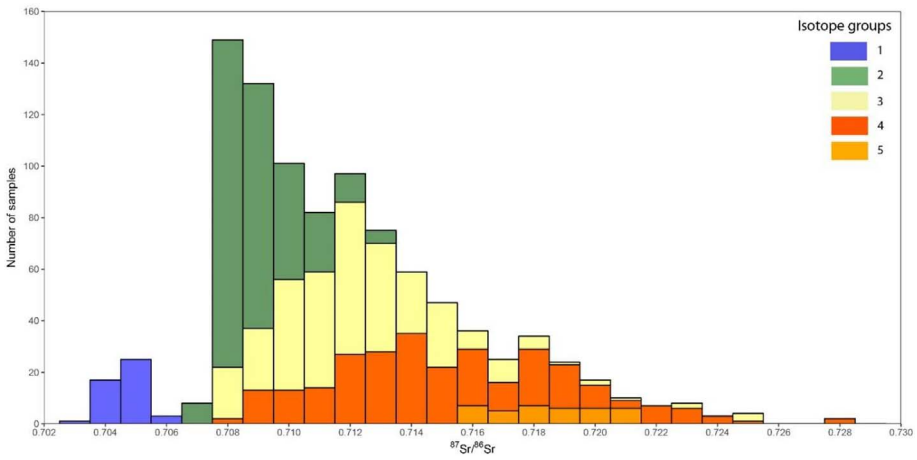

Fig. 6. Histogram of $^{87}Sr/^{86}Sr$ ratios from soil and plant samples, coloured by isotope group.

Table 3
Kriging method parameters.

Method	Transformation	Trend removal	Variogram model	Search Neighbourhood	Sectors	RMSE
Ordinary kriging	None	None	Exponential	Standard Min: 5 Max: 50	4	Soils: 0.00308 Plants: 0.00318
Kriging with External Drift	None	Constant	Exponential	Standard Min: 5 Max: 50	4	Soils: 0.00290 Plants: 0.00289

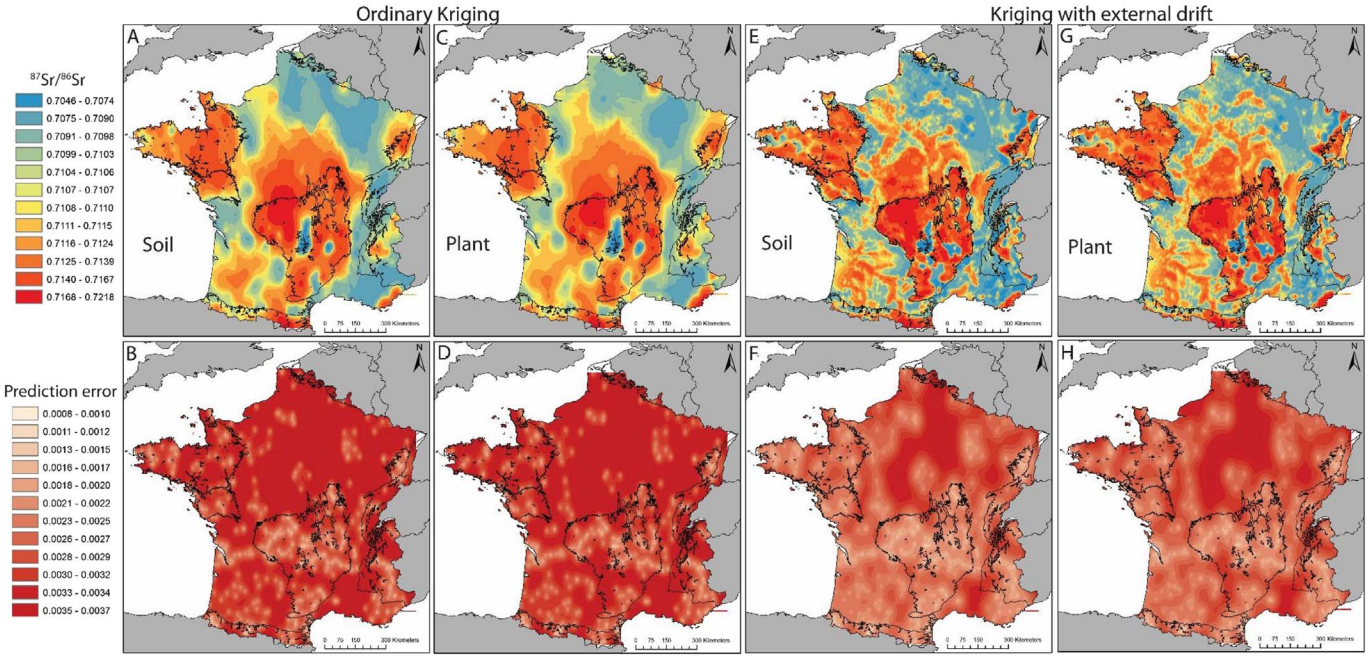

Fig. 7. Results from ordinary kriging for soils (A, B) and plants (C, D) and kriging with external drift for soil (E, F) and plants (G, H). No significant differences are observed between soil and plant samples. Kriging with external drift outperforms ordinary kriging and produces significantly lower prediction errors. High prediction errors remain in areas of low sample density.

with external drift using the geological cluster map as a covariate for both soil and plant samples (Fig. 7). Ordinary kriging resulted in a root-mean-square error (RMSE) of 0.0032 for soils and 0.0031 for plant samples. Kriging with external drift gave an improved RMSE with 0.0029 for both sample types. In addition, the use of the isotope groups as covariate in the kriging with external produces a strontium isoscape that more closely reflects the expected pattern of $^{87}Sr/^{86}Sr$ variations (Bataille and Bowen, 2012). Discrete $^{87}Sr/^{86}Sr$ variations following geological clusters dominate at large spatial scale whereas more continuous intra-unit variations reflect local geochemical heterogeneity. This pattern of $^{87}Sr/^{86}Sr$ variations is in contrast with the continuous $^{87}Sr/^{86}Sr$ variations produced by ordinary kriging which can only map $^{87}Sr/^{86}Sr$ variations as broad gradients with prediction rapidly deteriorating away from the bioavailable sampling sites. The pattern also differs from the $^{87}Sr/^{86}Sr$ cluster map by accounting for the intra-unit variability and by smoothing the discrete geological boundaries in the $^{87}Sr/^{86}Sr$ variability. The increase in prediction conformity with the current knowledge of Sr cycling is also visible when looking at individual transect of $^{87}Sr/^{86}Sr$ predictions through France. The map produced using kriging with external drift shows rapid shift of $^{87}Sr/^{86}Sr$ values at geological boundaries (e.g. Massif Central vs. sedimentary basins) as well as more diffuse boundaries associated with geomorphological processes (e.g. river valleys). River valleys accumulate sediments from isotopically distinct parent rocks which differ from the local bedrock $^{87}Sr/^{86}Sr$ values. For instance, the Loire, Garonne, or Seine rivers display higher $^{87}Sr/^{86}Sr$ values than the surrounding rock units because they are transporting sediments from older radiogenic rock units upstream.

Advantageously, kriging also provides estimates of spatial uncertainty which is critical to integrate $^{87}Sr/^{86}Sr$ models in quantitative framework of geographic assignment (Wunder, 2012). The RMSE value of 0.0029 (12% of the whole $^{87}Sr/^{86}Sr$ dataset range) for kriging with external drift for the combined soil and plant dataset demonstrates that significant uncertainty remains in predicting $^{87}Sr/^{86}Sr$ variations and would significantly limit quantitative geographic assignment efforts. However, when comparing the spatial uncertainty map generated by ordinary kriging and kriging with external drift, the variance is significantly reduced in the kriging with external drift. The ordinary kriging variance shows a bullseye pattern, centred around sampling sites, that is heavily dependent on the range of the fitted variogram model with prediction becoming rapidly uncertain away from the points. Conversely, the kriging with external drift shows much lower variance away from the point as it integrates both the predictive potential of the bioavailable dataset and that of the covariate. While this spatial uncertainty is markedly reduced, the kriging variance remains high in areas with very low sampling density (e.g. Paris Basin and Rhone delta). Additional sampling coupled with improved geostatistical framework to incorporate existing geospatial covariates would further improve the accuracy and resolution of those models. As a summary, the kriging with geological clusters as external drift produces a more detailed and realistic strontium isotope map of France than either the isotope group methods or the ordinary kriging methods. Those methods are, to date, the two most commonly applied methods to map $^{87}Sr/^{86}Sr$ variations (Copeland et al., 2016; Evans et al., 2010; Hodell et al., 2004). Our method proposes to combine these previous approaches in a two-step process to reach higher predictive power.

3.4. Application to archaeological provenance studies

France exhibits a significant contrast in $^{87}Sr/^{86}Sr$ ratios making it a suitable area to apply strontium isotopes for archaeological provenance studies (Fig. 8). The map produced in this study represents the first large scale bioavailable $^{87}Sr/^{86}Sr$ baseline for all of France and provides a powerful new tool for archaeological studies when taking the following limitations into account.

(1) The sample density is low given the large geographic area of France and only covers major geologic units. Increasing sample density will likely resolve finer scale patterns of strontium isotopic variation across the landscape. The prediction error maps (Fig. 7F, H) provide a direct indication of where additional samples are needed to improve this map, mainly the northern border of the Massif Central and the Paris Basin.
(2) The large $^{87}Sr/^{86}Sr$ ranges found in many lithological units and isotope groups, and the occurrence of similar lithological units with overlapping $^{87}Sr/^{86}Sr$ ranges at geographically distant areas in

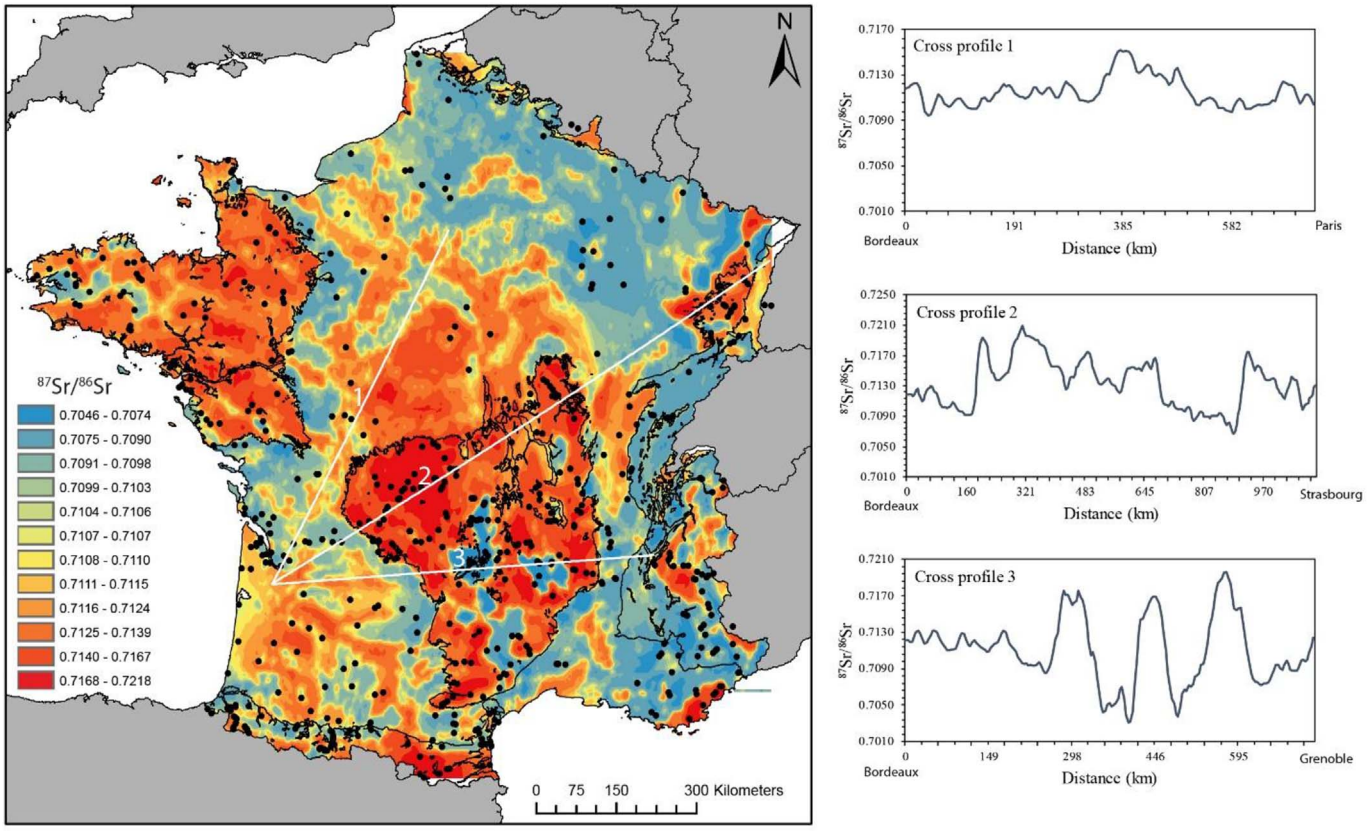

Fig. 8. Strontium isoscape of France based on combined soil and plant samples with kriging with external drift. Three example cross profiles are shown (white lines), originating from Bordeaux and going to Paris (Cross profile 1), Strasbourg (Cross profile 2), and Grenoble (Cross profile 3). Black dots represent the sample locations.

France may limit the identification of mobility and land-use between those areas. This is showcased in the three example cross profiles across France (Fig. 8). Along cross profile 1 (Bordeaux to Paris), many geographically distant areas have similar $^{87}Sr/^{86}Sr$ ratios, which would limit the identification of mobility along this vector. On the other hand, cross profile 2 (Bordeaux to Strasbourg) and cross profile 3 (Bordeaux to Grenoble), cross the Massif Central and exhibit many geographically distinct $^{87}Sr/^{86}Sr$ ratios, which would allow for a detailed investigation of mobility across this landscape. The sequence and timing of the $^{87}Sr/^{86}Sr$ ratios can further help identify mobility patterns, when it can be retrieved from the skeletal material, by for example multiple teeth from a single individual or using in-situ methods to extract time resolved information from a sample.

(3) The extent of the strontium baseline map is constrained to present day France, which creates boundaries with no significant meaning for many archaeological provenance studies. This can be overcome by including other strontium isotope baseline maps and detailed local studies into the analysis. This is facilitated by founding the baseline map on the surface geologic map of Europe, which uses consistent lithological identifiers across all of Europe and sharing the data on the IRHUM database (Willmes et al., 2014).

(4) Another limitation of the baseline map presented here is caused by the use of modern environmental samples. For example, the last ice age has significantly influenced the distribution of surface deposits in many parts of Europe and this needs to be considered when applying a map like this to trace human mobility and land-use in the distant past. The spatial distribution of exogenous surface deposits (Scheib et al., 2014) could be used to identify problematic areas that may have been significantly altered in recent geological time. In addition, climatological and atmospheric conditions change and thus could have a temporally variable effect on the strontium isotope ratios measured in plants and soils. Modern samples that are affected by anthropogenic influences are problematic in this regard and need to be avoided for the creation of a baseline map for archaeological provenance studies. Care was taken during sample selection to avoid these areas using information from the GEMAS (Reimann et al., 2014) and CORINE land use dataset (European Environment Agency (EEA), 2009).

(5) An additional limitation of this map is that it does not take atmospheric deposition of strontium into account to delineate different isotopic regions. The atmospheric deposition of strontium from precipitation, sea spray, and dust can have a significant contribution to the $^{87}Sr/^{86}Sr$ ratios of plants and soils in France. Due to their spatially and temporally complex patterns it was not possible to quantify their contribution to the bioavailable $^{87}Sr/^{86}Sr$ ranges for the lithological units in this study. Thus, the $^{87}Sr/^{86}Sr$ ranges established in this map may not adequately reflect times of greatly different climatological and atmospheric regimes in the past.

(6) Similarly, anthropogenic inputs of strontium are not considered in this map. Samples were selected from sites that should minimize these inputs, nevertheless in a country such as France anthropogenic inputs are likely and not always identifiable in the field. Artificial fertilizers and soil amendments are commonly used in Europe and may contribute a significant component to the Sr content in soil and plant material. Only very restricted information is available on the Sr concentration and isotopic composition of artificial fertilizers. A comprehensive study of fertilizers in Spain (Vitòria et al., 2004) found that there is a large variation in $^{87}Sr/^{86}Sr$ ratios for different fertilizers spanning most of the geological materials on Earth. Most fertilizers showed $^{87}Sr/^{86}Sr$ ratios around 0.708–0.709 thus overlapping with modern seawater compositions. However, depending on their source, fertilizers can have highly variable Sr concentrations and $^{87}Sr/^{86}Sr$ ratios. Other

anthropogenic sources are urban and industrial wastes ~0.708 and detergents ~0.709–0.710 (Vitòria et al., 2004). A case study investigating the Allanche river watershed in the Massif Central found that while there was a high fertilizer input of dissolved major ions, the Sr source was dominated (~90%) by bedrock weathering (Négrel and Deschamps, 1996). Studies of stream and ground water in the mountainous areas of France such as Armorican Massif and Massif Central have found variable influence of fertilizers and have related generally low $^{87}Sr/^{86}Sr$ ratios to manure from livestock farming (0.7092–0.7109) and fertilizer application (0.7079–0.7095) (Négrel, 1999; Négrel et al., 2004). Data from the GEMAS atlas do not show a systematic and significant difference between the extractable Sr content of agricultural or grazing soils (Reimann et al., 2014), indicating that fertilizer application might not be a major source of Sr for soils in many areas in France.

We recommend using this map (Fig. 8) in combination with detailed strontium isotopic studies around the archaeological site in question. In this capacity, it provides a powerful tool to identify possible residence and food source areas. For the application to provenance human or animal remains we can make use of the fact that these animals will average their food source over a geographic area and time. Thus, more extreme $^{87}Sr/^{86}Sr$ values are less likely to contribute significantly, increasing our ability to identify different regions and thus allowing a more nuanced interpretation of the data. The map is also a useful tool to determine where strontium isotopic tracing studies should best be applied and what kind of geographic resolution can be expected.

4. Conclusions

This study presents the first bioavailable $^{87}Sr/^{86}Sr$ baseline map based on kriging with external drift, as a tool for archaeological provenance studies in France. The resulting map combines the strengths of discrete classification and geostatistical models and provides accurate $^{87}Sr/^{86}Sr$ predictions with a geologically and sample density informed estimate of spatial uncertainty. While this map presents a significant step forward in generating accurate $^{87}Sr/^{86}Sr$ isoscapes, the high remaining uncertainty also demonstrates that fine-modelling of $^{87}Sr/^{86}Sr$ variability is challenging and requires more than geological maps for accurately predicting $^{87}Sr/^{86}Sr$ variations on the surface. More in-depth studies are needed to quantify the spatial and temporal variability of the input from different strontium reservoirs into soils and plants which is the likely source of the observed offsets between sample types at a number of sample locations. Future studies should focus on increasing sampling density, developing predictive models and apply novel geostatistical frameworks to further quantify and predict the processes that lead to $^{87}Sr/^{86}Sr$ variability across the landscape. Finally, combining the $^{87}Sr/^{86}Sr$ isoscape map with additional isotopic and elemental tracers (such as oxygen and lead) could further constrain the vector and distance of mobility and facilitate more nuanced archaeological interpretations.

Acknowledgements

We thank Bruno Maureille, Maxime Aubert, Patrice Courtaud, Christophe Falguères, Graham Mortimer, Philippe Rossi, Ceridwen Boel, Magdalena Huyskens, Eric Ward, and Nigel Craddy for their unwavering support with this project. Funding was provided by ARC DP110101415 (Grün, Spriggs, Armstrong, Maureille and Falguères) *Understanding the migrations of prehistoric populations through direct dating and isotopic tracking of their mobility patterns*. Part of this research was supported by the Australian French Association for Science & Technology through the ACT Science Fellowship program (2013) to M. Willmes. The authors thank the four anonymous reviewers whose constructive and thorough critique significantly improved the quality of this manuscript.

References

Bataille, C.P., Bowen, G.J., 2012. Mapping $^{87}Sr/^{86}Sr$ variations in bedrock and water for large scale provenance studies. Chem. Geol. 304–305, 39–52. http://dx.doi.org/10.1016/j.chemgeo.2012.01.028.

Bataille, C.P., Brennan, S.R., Hartmann, J., Moosdorf, N., Wooller, M.J., Bowen, G.J., 2014. A geostatistical framework for predicting variations in strontium concentrations and isotope ratios in Alaskan rivers. Chem. Geol. 389, 1–15. http://dx.doi.org/10.1016/j.chemgeo.2014.08.030.

Bataille, C.P., Laffoon, J., Bowen, G.J., 2012. Mapping multiple source effects on the strontium isotopic signatures of ecosystems from the circum-Caribbean region. Ecosphere 3, 1–24. http://dx.doi.org/10.1890/ES12-00155.1.

Beard, B.L., Johnson, C.M., 2000. Strontium isotope composition of skeletal material can determine the birth place and geographic mobility of humans and animals. J. Forensic Sci. 45, 1049–1061.

Bentley, R.A., 2006. Strontium isotopes from the earth to the archaeological skeleton: a review. J. Archaeol. Meth. Theor 13, 135–187. http://dx.doi.org/10.1007/s10816-006-9009-x.

Blum, J.D., Taliaferro, E.H., Weisse, M.T., Holmes, R.T., 2000. Changes in Sr/Ca, Ba/Ca and $^{87}Sr/^{86}Sr$ ratios between trophic levels in two forest ecosystems in the northeastern U.S.A. Biogeochemistry 49, 87–101. http://dx.doi.org/10.1023/A:1006390707989.

Brennan, S.R., Fernandez, D.P., Mackey, G., Cerling, T.E., Bataille, C.P., Bowen, G.J., Wooller, M.J., 2014. Strontium isotope variation and carbonate versus silicate weathering in rivers from across Alaska: implications for provenance studies. Chem. Geol. 389, 167–181. http://dx.doi.org/10.1016/j.chemgeo.2014.08.018.

BRGM, n.d. Geology of France at 1:1million scale (sixth edition) - OneGeology-Europe project - WP6.

Brock, G., Pihur, V., Datta, S., Datta, S., 2008. clValid: an R package for cluster validation. J. Stat. Software 25, 1–22.

Capo, R.C., Stewart, B.W., Chadwick, O.A., 1998. Strontium isotopes as tracers of ecosystem processes: theory and methods. Geoderma 82, 197–225. http://dx.doi.org/10.1016/S0016-7061(97)00102-X.

Chantraine, J., Chêne, F., Nehlig, P., Rabu, D., 2005. Carte géologique de la France à 1/1 000 000 6e édition révisée 2003. BRGM.

Copeland, S.R., Cawthra, H.C., Fisher, E.C., Lee-Thorp, J.A., Cowling, R.M., le Roux, P.J., Hodgkins, J., Marean, C.W., 2016. Strontium isotope investigation of ungulate movement patterns on the pleistocene paleo-agulhas plain of the greater cape floristic region, South Africa. Quat. Sci. Rev. 141, 65–84. http://dx.doi.org/10.1016/j.quascirev.2016.04.002.

Drouet, T., Herbauts, J., Gruber, W., Demaiffe, D., 2007. Natural strontium isotope composition as a tracer of weathering patterns and of exchangeable calcium sources in acid leached soils developed on loess of central Belgium. Eur. J. Soil Sci. 58, 302–319. http://dx.doi.org/10.1111/j.1365-2389.2006.00840.x.

European Environment Agency (EEA), 2009. Corine Land Cover.

Evans, J.A., Montgomery, J., Wildman, G., 2009. Isotope domain mapping of $^{87}Sr/^{86}Sr$ biosphere variation on the Isle of Skye. Scotland. J. Geol. Soc. London 166, 617–631. http://dx.doi.org/10.1144/0016-76492008-043.

Evans, J.A., Montgomery, J., Wildman, G., Boulton, N., 2010. Spatial variations in biosphere $^{87}Sr/^{86}Sr$ in Britain. J. Geol. Soc. London 167, 1–4. http://dx.doi.org/10.1144/0016-76492009-090.

Evans, J.A., Tatham, S., 2004. In: Defining "local Signature" in Terms of Sr Isotope Composition Using a Tenth- to Twelfth-century Anglo-saxon Population Living on a Jurassic Clay-carbonate Terrain, vol. 232. Geol. Soc. London, Rutland, UK, pp. 237–248. http://dx.doi.org/10.1144/GSL.SP.2004.232.01.21. Spec. Publ.

Faure, G., Mensing, T.M., 2005. Isotopes: Principles and Applications, third ed. John Wiley and Sons Inc., Hoboken, New Jersey.

Frei, K.M., Frei, R., 2011. The geographic distribution of strontium isotopes in Danish surface waters – a base for provenance studies in archaeology, hydrology and agriculture. Appl. Geochem. 26, 326–340. http://dx.doi.org/10.1016/j.apgeochem.2010.12.006.

Frei, R., Frei, K.M., 2013. The geographic distribution of Sr isotopes from surface waters and soil extracts over the island of Bornholm (Denmark) - a base for provenance studies in archaeology and agriculture. Appl. Geochem. 38, 147–160. http://dx.doi.org/10.1016/j.apgeochem.2013.09.007.

Goovaerts, P., 1998. Ordinary cokriging revisited 1. Math. Geol. 30, 21–42. http://dx.doi.org/10.1023/A:1021757104135.

Gryschko, R., Kuhnle, R., Terytze, K., Breuer, J., Stahr, K., 2005. Research articles soil extraction of readily soluble heavy metals and as with 1 M NH_4NO_3-solution. J. Soils Sediments 5, 101–106. http://dx.doi.org/10.1065/jss2004.10.119.

Hall, G.E.M., Maclaurin, A.I., Garrett, R.G., 1998. Assessment of the 1 M NH_4NO_3 extraction protocol to identify mobile forms of Cd in soils. J. Geochem. Explor. 64, 153–159.

Hartman, G., Richards, M., 2014. Mapping and defining sources of variability in bioavailable strontium isotope ratios in the Eastern Mediterranean. Geochem. Cosmochim. Acta 126, 250–264. http://dx.doi.org/10.1016/j.gca.2013.11.015.

Hennig, C., 2015. fpc: Flexible Procedures for Clustering. R Package Version 2.1-10.

Hobbs, J.A., Yin, Q., Burton, J., Bennett, W.A., 2005. Retrospective determination of natal habitats for an estuarine fish with otolith strontium isotope ratios. Mar. Freshw. Res. 56, 655. http://dx.doi.org/10.1071/MF04136.

Hodell, D.A., Quinn, R.L., Brenner, M., Kamenov, G., 2004. Spatial variation of strontium isotopes ($^{87}Sr/^{86}Sr$) in the Maya region: a tool for tracking ancient human migration. J. Archaeol. Sci. 31, 585–601. http://dx.doi.org/10.1016/j.jas.2003.10.009.

Kelly, S., Heaton, K., Hoogewerff, J., 2005. Tracing the geographical origin of food: the application of multi-element and multi-isotope analysis. Trends Food Sci. Technol.

16, 555–567. http://dx.doi.org/10.1016/j.tifs.2005.08.008.
Kootker, L.M., van Lanen, R.J., Kars, H., Davies, G.R., 2016. Strontium isoscapes in The Netherlands. Spatial variations in $^{87}Sr/^{86}Sr$ as a proxy for palaeomobility. J. Archaeol. Sci. Reports 6, 1–13. http://dx.doi.org/10.1016/j.jasrep.2016.01.015.
Krige, D.G., 1951. A Statistical Approach to Some Basic Mine Valuation Problems on the Witwatersrand. University of Witwatersrandhttp://dx.doi.org/10.2307/3006914.
Laffoon, J.E., Davies, G.R., Hoogland, M.L.P., Hofman, C.L., 2012. Spatial variation of biologically available strontium isotopes ($^{87}Sr/^{86}Sr$) in an archipelagic setting: a case study from the Caribbean. J. Archaeol. Sci. 39, 2371–2384. http://dx.doi.org/10.1016/j.jas.2012.02.002.
Maechler, M., Rousseeuw, P., Struyf, A., Hubert, M., Hornik, K., 2015. Cluster: Cluster Analysis Basics and Extensions. R Package Version 2.0.3.
Maurer, A.F., Galer, S.J.G., Knipper, C., Beierlein, L., Nunn, E.V., Peters, D., Tütken, T., Alt, K.W., Schöne, B.R., 2012. Bioavailable $^{87}Sr/^{86}Sr$ in different environmental samples - effects of anthropogenic contamination and implications for isoscapes in past migration studies. Sci. Total Environ. 433, 216–229. http://dx.doi.org/10.1016/j.scitotenv.2012.06.046.
Meers, E., Du Laing, G., Unamuno, V., Ruttens, A., Vangronsveld, J., Tack, F.M.G., Verloo, M.G., 2007. Comparison of cadmium extractability from soils by commonly used single extraction protocols. Geoderma 141, 247–259. http://dx.doi.org/10.1016/j.geoderma.2007.06.002.
Négrel, P., 1999. Geochemical study of a granitic area – the MargerideMountains, France: chemical element behavior and $^{87}Sr/^{86}Sr$ constraints. Aquat. Geochem. 5, 125–165. http://dx.doi.org/10.1023/A:1009625412015.
Négrel, P., Deschamps, P., 1996. Natural and anthropogenic budgets of a small watershed in the massif central (France): chemical and strontium isotopic characterization of water and sediments. Aquat. Geochem. 2, 1–27. http://dx.doi.org/10.1007/BF00240851.
Négrel, P., Petelet-Giraud, E., Widory, D., 2004. Strontium isotope geochemistry of alluvial groundwater: a tracer for groundwater resources characterisation. Hydrol. Earth Syst. Sci. 8, 959–972. http://dx.doi.org/10.5194/hess-8-959-2004.
Pestle, W.J., Simonetti, A., Curet, L.A., 2013. $^{87}Sr/^{86}Sr$ variability in Puerto Rico: geological complexity and the study of paleomobility. J. Archaeol. Sci. 40, 2561–2569. http://dx.doi.org/10.1016/j.jas.2013.01.020.
Poszwa, A., Dambrine, E., Ferry, B., Pollier, B., Loubet, M., 2002. Do deep tree roots provide nutrients to the tropical rainforest? Biogeochemistry 60, 97–118. http://dx.doi.org/10.1023/A:1016548113624.
Poszwa, A., Ferry, B., Dambrine, E., Pollier, B., Wickman, T., Loubet, M., Bishop, K., 2004. Variations of bioavailable Sr concentration and $^{87}Sr/^{86}Sr$ ratio in boreal forest ecosystems: role of biocycling, mineral weathering and depth of root uptake. Biogeochemistry 67, 1–20. http://dx.doi.org/10.1023/B: BIOG.0000015162.12857.3e.
Price, T.D., Burton, J.H.H., Bentley, R.A., 2002. The characterization of biologically available strontium isotope ratios for the study of prehistoric migration. Archaeometry 44, 117–135. http://dx.doi.org/10.1111/1475-4754.00047.
Price, T.D., Knipper, C., Grupe, G., Smrcka, V., 2004. Strontium isotopes and prehistoric human migration: the bell beaker period in central europe. Eur. J. Archaeol. 7, 9–40. http://dx.doi.org/10.1177/1461957104047992.
Prohaska, T., Wenzel, W.W., Stingeder, G., 2005. ICP-MS-based tracing of metal sources and mobility in a soil depth profile via the isotopic variation of Sr and Pb. Int. J. Mass Spectrom. 242, 243–250. http://dx.doi.org/10.1016/j.ijms.2004.11.028.
R Core Team, 2017. R: a Language and Environment for Statistical Computing.
Rao, C.R.M., Sahuquillo, A., Lopez Sanchez, J.F., 2008. A review of the different methods applied in environmental geochemistry for single and sequential extraction of trace elements in soils and related materials. Water Air Soil Pollut. http://dx.doi.org/10.1007/s11270-007-9564-0.
Reimann, C., Birke, M., Demetriades, A., Filzmoser, P., O'Connor, P., O'Connor, P., 2014. Chemistry of Europe's Agricultural Soils. Part a: Methodology and Interpretation of the GEMAS Data Set.
Saby, N., Arrouays, D., Boulonne, L., Jolivet, C., Pochot, A., 2006. Geostatistical assessment of Pb in soil around Paris. France. Sci. Total Environ. 367, 212–221. http://dx.doi.org/10.1016/j.scitotenv.2005.11.028.
Scheib, A.J., Birke, M., Dinelli, E., GEMAS Project Team, 2014. Geochemical evidence of aeolian deposits in European soils. Boreas 43, 175–192. http://dx.doi.org/10.1111/bor.12029.
Sillen, A., Hall, G., Richardson, S., Armstrong, R., 1998. $^{87}Sr/^{86}Sr$ ratios in modern and fossil food-webs of the Sterkfontein Valley: implications for early hominid habitat preference. Geochem. Cosmochim. Acta 62, 2463–2473. http://dx.doi.org/10.1016/S0016-7037(98)00182-3.
Slovak, N.M., Paytan, A., 2012. Handbook of Environmental Isotope Geochemistry, Handbook of Environmental Isotope Geochemistry. Springer, Berlin, Heidelberg. http://dx.doi.org/10.1007/978-3-642-10637-8.
Song, B.-Y., Ryu, J.-S., Shin, H.S., Lee, K.-S., 2014. Determination of the source of bioavailable Sr using $^{87}Sr/^{86}Sr$ tracers: a case study of hot pepper and rice. J. Agric. Food Chem. 62, 9232–9238. http://dx.doi.org/10.1021/jf503498r.
Vitòria, L., Otero, N., Soler, A., Canals, A., 2004. Fertilizer characterization: isotopic data (N, S, O, C, and Sr). Environ. Sci. Technol. 38, 3254–3262.
Voerkelius, S., Lorenz, G.D., Rummel, S., Quétel, C.R., Heiss, G., Baxter, M., Brach-Papa, C., Deters-Itzelsberger, P., Hoelzl, S., Hoogewerff, J., Ponzevera, E., Van Bocxstaele, M., Ueckermann, H., 2010. Strontium isotopic signatures of natural mineral waters, the reference to a simple geological map and its potential for authentication of food. Food Chem. 118, 933–940. http://dx.doi.org/10.1016/j.foodchem.2009.04.125.
West, J.B., Bowen, G.J., Dawson, T.E., Tu, K.P., 2010. Isoscapes: understanding movement, pattern, and process on earth through isotope mapping. In: West, J.B., Bowen, G.J., Dawson, T.E., Tu, K.P. (Eds.), Isoscapes: Understanding Movement, Pattern, and Process on Earth through Isotope Mapping. Springer Netherlands, pp. 1–487. http://dx.doi.org/10.1007/978-90-481-3354-3.
Widga, C., Walker, J.D., Boehm, A., 2017. Variability in bioavailable $^{87}Sr/^{86}Sr$ in the north american midcontinent. Open Quat. 3, 4. http://dx.doi.org/10.5334/oq.32.
Willmes, M., McMorrow, L., Kinsley, L., Armstrong, R.A., Aubert, M., Eggins, S., Falguères, C., Maureille, B., Moffat, I., Grün, R., 2014. The IRHUM (Isotopic Reconstruction of Human Migration) database – bioavailable strontium isotope ratios for geochemical fingerprinting in France. Earth Syst. Sci. Data 6, 117–122. http://dx.doi.org/10.5194/essd-6-117-2014.
Wunder, M.B., 2012. Determining geographic patterns of migration and dispersal using stable isotopes in keratins. J. Mammal. 93, 360–367. http://dx.doi.org/10.1644/11-MAMM-S-182.1.